Hindawi Publishing Corporation
Journal of Nanomaterials
Volume 2013, Article ID 751826, 6 pages
http://dx.doi.org/10.1155/2013/751826

Research Article

Y-Doped ZnO Nanorods by Hydrothermal Method and Their Acetone Gas Sensitivity

Peng Yu,[1] Jing Wang,[1] Hai-ying Du,[1,2] Peng-jun Yao,[1,3] Yuwen Hao,[1] and Xiao-gan Li[1]

[1] *School of Electronic Science and Technology, Dalian University of Technology, Dalian, Liaoning 116023, China*
[2] *Department of Electromechanical Engineering and Information, Dalian Nationalities University, Dalian, Liaoning 116600, China*
[3] *School of Educational Technology, Shenyang Normal University, Shenyang, Liaoning 110000, China*

Correspondence should be addressed to Jing Wang; wangjing@dlut.edu.cn

Received 21 October 2013; Accepted 9 December 2013

Academic Editor: Xiangyu Zhao

Pure and yttrium- (Y-) doped (1 at%, 3 at%, and 7 at%) ZnO nanorods were synthesized using a hydrothermal process. The crystallography and microstructure of the synthesized samples were characterized by X-ray diffraction (XRD), scanning electron microscopy (SEM), and energy dispersive X-ray spectroscopy (EDX). Comparing with pure ZnO nanorods, Y-doped ZnO exhibited improved acetone sensing properties. The response of 1 at% Y-doped ZnO nanorods to 100 ppm acetone is larger than that of pure ZnO nanorods. The response and recovery times of 1 at% Y-doped ZnO nanorods to 100 ppm acetone are about 30 s and 90 s, respectively. The gas sensor based on Y-doped ZnO nanorods showed good selectivity to acetone in the interfere gases of ammonia, benzene, formaldehyde, toluene, and methanol. The formation mechanism of the ZnO nanorods was briefly analyzed.

1. Introduction

As an important II–VI semiconducting material with a wide direct band gap (E_g = 3.37 eV at 300 K) and large exciton binding energy (~60 meV), ZnO has drawn much attention in the last few decades, owing to its specific electrical, catalytic, photochemical optoelectronic properties and the sensitivity to various gases, all of which make ZnO highly promising in a broad range of real-world applications [1, 2]. Recently, ZnO has shown great potentials for sensing toxic and combustible gases such as CO, H_2, NH_3, ethanol, and acetone [3–5].

One way to enhance gas sensing property is by doping with other elements. For example, Niu et al. [6] used Fe, Co, and Cr as dopants to improve the gas sensing property of pure ZnO, and the results showed that $ZnFe_2O_4$ had high response and good selectivity to Cl_2. Au-doped ZnO enhanced acetone sensing performance [7]. Co-doped ZnO nanofibers improved selective acetone sensing properties [8]. Pd [9] is also used as dopant to improve CO gas sensing property of ZnO. There are some reports about the lanthanide elements of Y-doped ZnO and Y doping has significant effects on the luminescence, chemical, and surface modification of ZnO [10, 11]. However, the lanthanide elements of Y as a dopant to improve gas sensing property of ZnO are new challenges. Furthermore, many synthesis methods have been used to prepare zinc-oxide nanoparticles (NPs) including chemical vapor deposition [12], sol-gel method [13], spray pyrolysis method [14], solid state reaction method [15], and hydrothermal method [16]. Hydrothermal method is fairly simple and suitable for industrial production, which will pave the way for the development of a low-cost practical gas sensor for detection of probable chemical agents.

In this paper, we report the synthesis and gas sensing properties of pure and Y-doped ZnO rods using a facile hydrothermal method. One at% Y-doped ZnO sensor exhibits improved acetone sensing properties. A possible explanation of sensing mechanism and the effects of Y doping on acetone sensing properties has been analyzed.

2. Experiments

2.1. Synthesis and Characterization of ZnO Nanorods. All the starting materials were analytical grade and were

used without further purification. Zinc nitrate hexahydrate ($Zn(NO_3)_2{\cdot}6H_2O$) and yttrium nitrate hexahydrate ($Y(NO_3)_3{\cdot}6H_2O$) were used as Zn and Y sources, respectively. The precipitate reagent was hexamethylene tetramine. ZnO seed layer was needed before the pure and Y-doped ZnO samples synthesis. In a typical procedure of seed layer preparation, 21.9 mg zinc acetate ($Zn(CH_3COO)_2{\cdot}2H_2O$) was dissolved in 50 mL deionized water to form a solution with concentration of 2 mM. And then the solution was ultrasonically agitated for 0.5 h to obtain a uniform and transparent zinc acetate solution. This solution was coated onto cleaned glass substrates by a spin coater at a rate of 2200 rpm for 30 s. The coated substrates were dried in room temperature and then annealed at 200°C for 1 h in air to yield a layer of ZnO seed on the substrate. And then the spin coat and anneal process were repeated two times.

In this process, 630 mg of $Zn(NO_3)_2{\cdot}6H_2O$ and certain amount of $Y(NO_3)_3{\cdot}6H_2O$ (0, 1 at%, 3 at%, and 7 at%) were dissolved in 30 mL deionized water. Subsequently, 297 mg of hexamethylenetetramine (HMTA: $C_6H_{12}N_4$) was dissolved into 30 mL deionized water in another beaker under vigorous stirring for 0.5 h. The pH of growth solution was ~6. After that, two solutions were mixed together under stirring and then the seeded glass substrates were immersed into the solution. Then the beaker was put into the oven and kept in it for 8 h at 95°C. After the beaker was cooled to room temperature naturally, the substrate was removed from the solution and washed with deionized water and absolute ethanol, respectively, four times. The ZnO rod powders were obtained after the samples were dried in air at 60°C.

X-ray diffraction (XRD) patterns of the powders were examined in 2θ region of 20°–80° with Cu $K\alpha$ (0.154 nm) radiation on Rigaku, Model D/M AX 2400, Japan. Scanning electron microscopy (SEM) images were examined on a FEI QUANTA 200F (USA) microscope equipped with energy dispersive X-ray (EDX) spectroscopy.

2.2. Sensor Fabrication and Gas Sensing Performance Test. A proper amount of ZnO materials was mixed with several drops of deionized water to form a paste. The paste was coated on a ceramic tube on which a pair of gold electrodes was previously printed, and then a Ni-Cr heating wire was inserted in the tube to form a gas sensor. The thickness of the sensing films was about 300 μm. The alumina tube was then welded onto a pedestal to form a final sensor unit. The sensors were aged at 300°C for ten days to achieve the stabilization. The gas sensing tests were operated in a static state gas sensing test system [17]. When the resistance of all the sensors was stable, target gas was injected into the test chamber by a microinjector through a rubber plug. After measurement, the sensor was exposed to air by opening the chamber to the atmosphere. The output voltages of the sensors were measured under a bias voltage of 10 V DC. The sensor response value (S) was defined as $S = R_a/R_g$, where R_a and R_g were the resistance of the sensor in air and in target gas, respectively. The time taken by the sensor to achieve 90% of the total resistance change was defined as the response time in the case of response (target gas adsorption) or the recovery time in the case of recovery (target gas desorption). The whole system was controlled by a computer automatically. All the tests were operated under about 30% relative humidity.

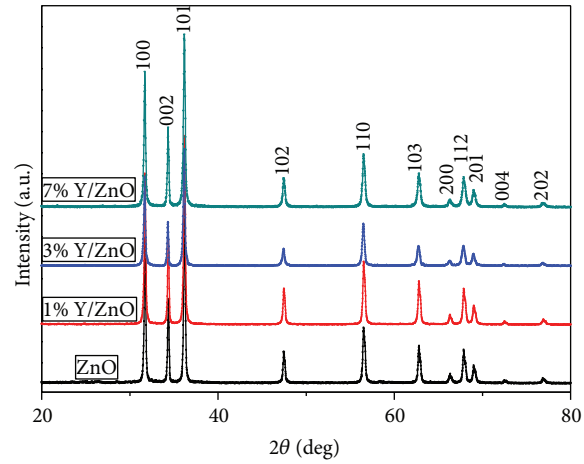

Figure 1: XRD patterns of pure, 1 at%, 3 at%, and 7 at% Y-doped ZnO nanorods.

3. Results and Discussion

3.1. Characterization Results and Growth Process Analysis of ZnO Nanorods. Figure 1 shows the XRD patterns of pure, 1 at%, 3 at%, and 7 at% Y-doped ZnO nanorods. The samples are polycrystalline in nature and no further heat treatment is required. All the diffraction peaks can be indexed as hexagonal ZnO with lattice constants $a = 0.325$ nm and $c = 0.521$ nm, which are consistent with the values in the standard card (Joint Committee for Powder Diffraction Studies (JCPDS) card # 36-1451).

Figure 2 shows the SEM images of the as-prepared nanorods with different Y doping rates: (a) pure, (b) 1 at%, (c) 3 at%, and (d) 7 at% Y-doped ZnO nanorods. The average diameters of pure, 1 at%, 3 at%, and 7 at% Y-doped ZnO nanorods are ~300 nm, 300 nm~1.5 μm, 2~3 μm, and 2~3 μm, respectively. It can be seen that the average diameters of the products are increased as the Y content increased from zero to 3 at%.

Figure 3 demonstrates the EDX analysis for the 1 at% Y-doped ZnO nanorods. We can see that the energy dispersive X-ray spectroscopic analysis confirmed the presence of Zn and Y elements in the investigated area from the Y-doped ZnO nanorods by a hydrothermal process.

The growth process of ZnO crystallites is generally accepted via the following mechanism [18–20]: HMTA ($C_6H_{12}N_4$) is extensively used in the synthesis of ZnO nanostructures, and it provides the ammonia molecules (NH_3) and the hydroxide ions (OH^-) to the solution (1) and (2). And $Zn(NO_3)_2{\cdot}6H_2O$ is apparently used to provide the zinc ions (3). In this experiment, OH^- is abundant in the mixed aqueous solution, fresh formed $Zn(OH)_2$ precipitation (4) can be dissolved immediately by reacting with superfluous OH^- ions, and then a transparent $Zn(OH)_4^{2-}$ solution is obtained (5). In the hydrothermal process, the $Zn(OH)_4^{2-}$

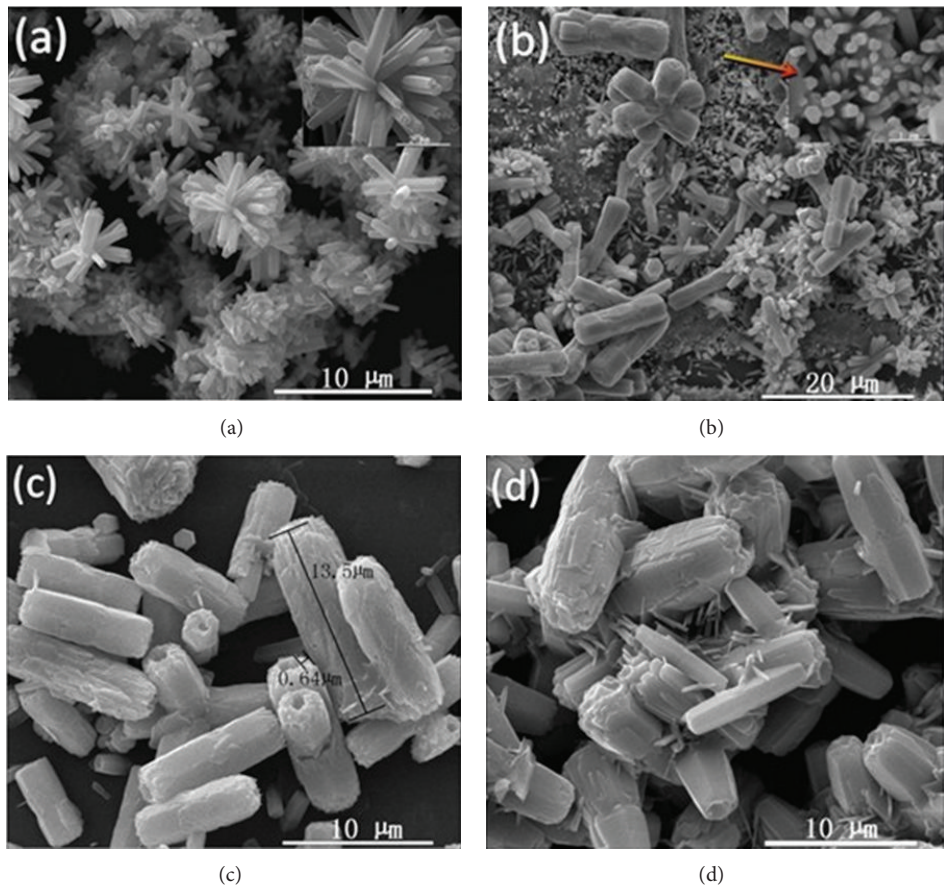

Figure 2: SEM images of (a) pure, (b) 1 at%, (c) 3 at%, and (d) 7 at% Y-doped ZnO nanorods.

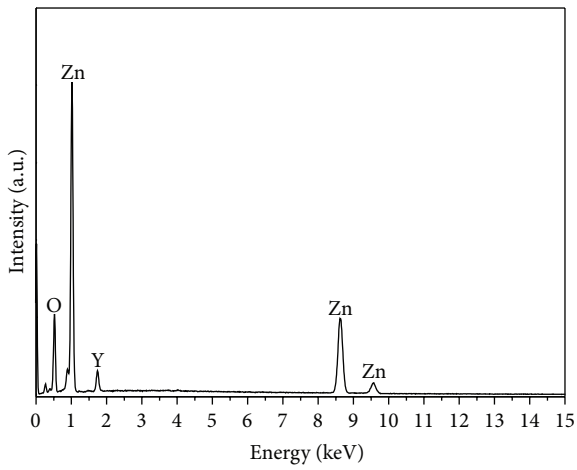

Figure 3: The EDX analysis of the 1 at% Y-doped ZnO nanorods.

combines with each other and dehydrates into ZnO nuclei simultaneously. And then these ZnO nuclei self-assemble to form the rod-like nanostructures along a preferred axis orientation (6):

$$C_6H_{12}N_4 + 6H_2O \longleftrightarrow 6HCHO + 4NH_3 \quad (1)$$

$$NH_3 + H_2O \longleftrightarrow NH_4^+ + OH^- \quad (2)$$

$$Zn(NO_3)_2 \longrightarrow Zn^{2+} + 2NO_3^- \quad (3)$$

$$Zn^{2+} + 2OH^- \longrightarrow Zn(OH)_2 \downarrow \quad (4)$$

$$Zn(OH)_2 + 2OH^- \longrightarrow Zn(OH)_4^{2-} \quad (5)$$

$$Zn(OH)_4^{2-} \longrightarrow ZnO + H_2O + 2OH^- \quad (6)$$

3.2. Gas Sensing Properties. Gas sensing properties were performed at different temperatures to find out the optimum operating condition for acetone detection. Figure 4 shows the responses of pure, 1 at%, 3 at%, and 7 at% Y-doped ZnO nanorods gas sensors to 100 ppm acetone vapor at different operating temperatures. The responses of all samples are found to increase with increasing the operating temperature, which attain the maximum at 400°C, and then decrease with a further rise of the operating temperature. This behavior can be explained from the kinetics and mechanics of gas adsorption and desorption on the surface of ZnO [21–24]. When the operating temperature is low, the chemical activation of nanorods is small, leading to a very small response. When the temperature is too high, some adsorbed gas molecules may escape before their reaction with the sensing material due to their enhanced activation; thus, the response will decrease correspondingly. At the optimal temperature of

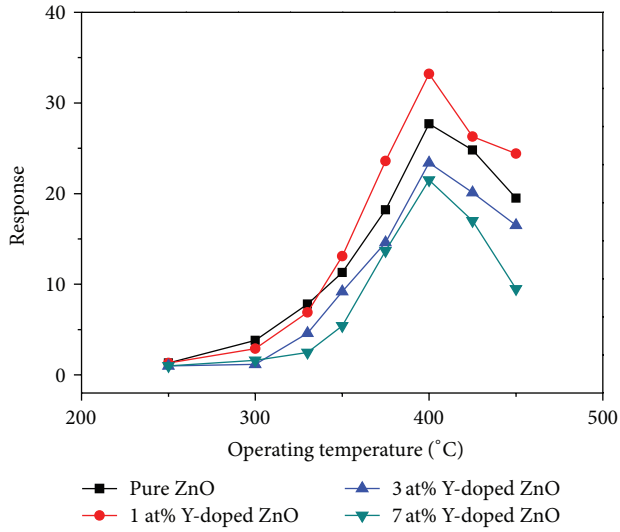

Figure 4: Responses of pure, 1 at%, 3 at%, and 7 at% Y-doped ZnO nanorods to 100 ppm acetone at different temperatures.

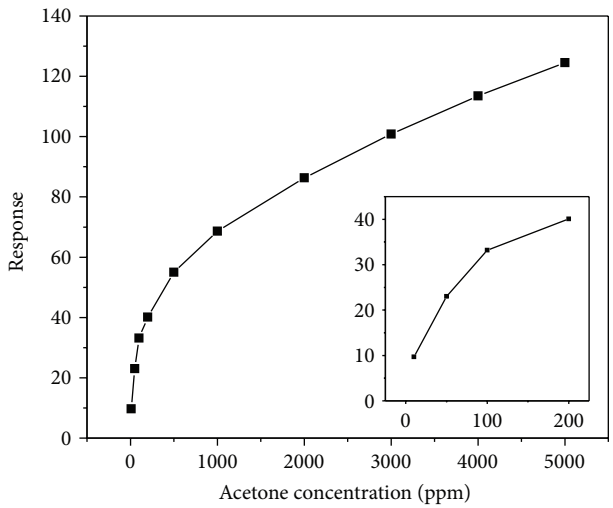

Figure 5: Responses of 1 at% Y-doped ZnO nanorods to different concentrations of acetone at 400°C; the insert shows the calibration curve in low concentration range.

400°C (corresponding to the maximum response), 1 at% Y-doped ZnO nanorods exhibit the highest response values. Thus, 1 at% Y-doped ZnO nanorods were applied in the entire investigations hereafter.

Figure 5 shows the sensor response versus acetone concentration at operating temperature 400°C, and the insert shows the calibration curve in low concentration range. We can see that the sensitivity (the slop of the curve) of the sensor is higher in low acetone concentration range than in high concentration range. The lowest concentration of the acetone that the sensor can detect is 10 ppm with the response value of 4.3.

The transient properties of 1 at% Y-doped ZnO nanorods sensor to different concentrations of acetone are shown in Figure 6. For acetone vapor at concentration levels of 100,

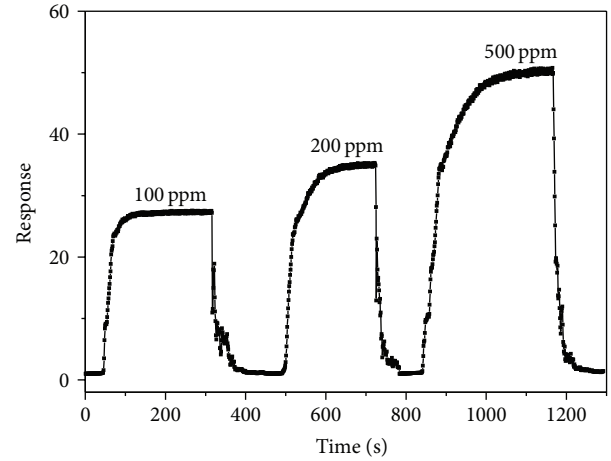

Figure 6: The transient property of 1 at% Y-doped ZnO nanorods sensor to 100, 200, and 500 ppm acetone consecutively.

200, and 500 ppm, the responses are about 33.2, 40.1, and 55, respectively. The response times are about 30 s, 34 s, and 42 s for 100 ppm, 200 ppm, and 500 ppm acetone, respectivily. Correspondingly, the recovery times are about 90 s, 100 s, and 115 s, respectively. As the concentration increases, the response time and the recovery time are both slightly increased. The sensor selectivity was tested by exposing it to 100 ppm different gases at operating temperature 400°C, as shown in Figure 7. We can see from Figure 7 that the sensor response to acetone (CH_3COCH_3) is higher than to ammonia (NH_3), benzene (C_6H_6), formaldehyde (HCHO), toluene ($C_6H_5CH_3$), and methanol (CH_3OH).

3.3. Gas Sensing Mechanism. For most semiconducting oxide gas sensor, the change in resistance is primarily caused by the adsorption and desorption of gas molecules on the surface of the sensing films [25, 26]. As a typical *n*-type MOS sensor, the ZnO based sensor belongs to the surface-controlled type [27]; namely, the sensor response is attributed to the chemisorptions of oxygen on the oxide surface and the subsequent reaction between adsorbed oxygen and tested gas, which brings the resistance of the sensing material change. In ambient air, ZnO nanorods adsorb the oxygen molecule on the surface. The adsorbed oxygen is changed to various chemical adsorptive states (O_2^-, O^{2-}, and O^-) by capturing electrons from the conductance band:

$$O_{2(g)} \Longleftrightarrow O_{2(ads)} \quad (7)$$

$$O_{2(ads)} + e^- \longrightarrow {O_{2(ads)}}^- \quad (8)$$

$${O_{2(ads)}}^- + e^- \longrightarrow 2O^-_{(ads)} \quad (9)$$

$$O^-_{(ads)} + e^- \longrightarrow O^{2-}_{(ads)} \quad (10)$$

Consequently, ZnO will show high resistance. According to the report by Takata et al. [28], the stable oxygen ions are O_2^- below 100°C, O^- between 100 and 300°C, and O^{2-} above 300°C. The operating temperature of the 1 at% Y-doped ZnO

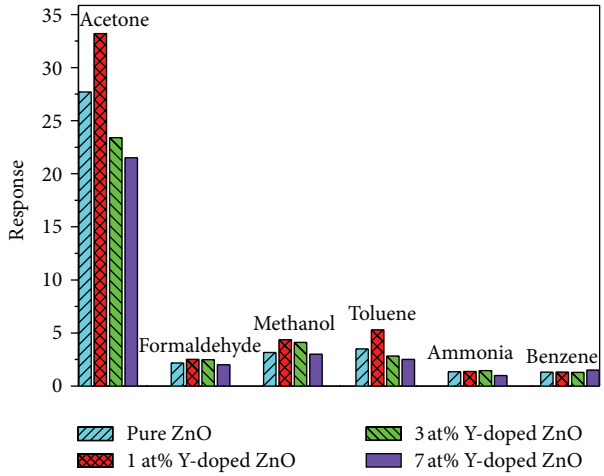

FIGURE 7: Responses of pure, 1 at%, 3 at%, and 7 at% Y-doped ZnO nanorods sensors to 100 ppm different gases.

nanorods sensor is 400°C, so O^{2-} is believed to be dominant state for adsorbed oxygen.

When ZnO is exposed to reductive gas acetone (CH_3COCH_3), the acetone molecules will react with adsorbed O^{2-} species on the ZnO surface to form CO_2 and H_2O, which leads to the increase of carrier concentration and the decrease of the electrical resistance:

$$CH_3COCH_{3(g)} + O^{2-}_{ads} \longrightarrow CO_{2(g)} + H_2O_{(g)} + 2e^- \quad (11)$$

As a catalyst, Y not only enhances the activity of the semiconductor surface, but also promotes the electrons transfer from the reducing gas (acetone vapor) to ZnO [8, 29]. On the other hand, impurity energy levels introduced by doping reduced the barrier height of ZnO [30]. When Y-doped ZnO nanorods are exposed to acetone vapor, its barrier height will become lower and depletion layer will be thinner, resulting in big changes of the resistance of the sensitive material. Therefore, the response of the Y-doped ZnO nanorods to acetone vapor increases. However, the samples with excess Y doping such as 7 at% deteriorate with worse response to acetone vapor (as shown in Figure 7). The mechanism of the gas response of ZnO doped with different concentration of Y also needs further investigation.

4. Conclusion

In summary, pure and Y-doped ZnO nanorods are synthesized via hydrothermal method. Gas sensing measurement reveals that Y doping can enhance the acetone sensing properties of ZnO nanorods, and the optimal doping concentration was 1 at%. The acetone vapor concentration ranges from 10 ppm to 5000 ppm. The response and recovery times of 1 at% Y-doped ZnO nanorods to 100 ppm acetone are about 30 s and 90 s, respectively. The sensor got good selectivity of acetone to ammonia, benzene, formaldehyde, toluene, and methanol. Doping yttrium into ZnO enhances the activity of the semiconductor surface and introduces impurity energy levels that reduce the barrier height of ZnO.

Acknowledgment

This paper was supported by the National Natural Science Foundation of China (61176068, 61131004, and 61001054).

References

[1] M. H. Huang, S. Mao, H. Feick et al., "Room-temperature ultraviolet nanowire nanolasers," *Science*, vol. 292, no. 5523, pp. 1897–1899, 2001.

[2] S.-H. Choi, G. Ankonina, D.-Y. Youn et al., "Hollow ZnO nanofibers fabricated using electrospun polymer templates and their electronic transport properties," *ACS Nano*, vol. 3, no. 9, pp. 2623–2631, 2009.

[3] Z. Yuan, X. Jiaqiang, X. Qun, L. Hui, P. Qingyi, and X. Pengcheng, "Brush-like hierarchical zno nanostructures: synthesis, photoluminescence and gas sensor properties," *Journal of Physical Chemistry C*, vol. 113, no. 9, pp. 3430–3435, 2009.

[4] A. K. Bai, A. Singh, and R. K. Bedi, "Characterization and ammonia sensing properties of pure and modified ZnO films," *Applied Physics A*, vol. 103, no. 2, pp. 497–503, 2011.

[5] S. K. Youn, N. Ramgir, C. Wang, K. Subannajui, V. Cimalla, and M. Zacharias, "Catalyst-free growth of ZnO nanowires based on topographical confinement and preferential chemisorption and their use for room temperature CO detection," *Journal of Physical Chemistry C*, vol. 114, no. 22, pp. 10092–10100, 2010.

[6] X. Niu, W. Du, and W. Du, "Preparation and gas sensing properties of ZnM2O4 (M = Fe, Co, Cr)," *Sensors and Actuators B*, vol. 99, no. 2-3, pp. 405–409, 2004.

[7] X.-J. Wang, W. Wang, and Y.-L. Liu, "Enhanced acetone sensing performance of Au nanoparticles functionalized flower-like ZnO," *Sensors and Actuators B*, vol. 168, pp. 39–45, 2012.

[8] L. Liu, S. Li, J. Zhuang et al., "Improved selective acetone sensing properties of Co-doped ZnO nanofibers by electrospinning," *Sensors and Actuators B*, vol. 155, no. 2, pp. 782–788, 2011.

[9] S. Wei, Y. Yu, and M. Zhou, "CO gas sensing of Pd-doped ZnO nanofibers synthesized by electrospinning method," *Materials Letters*, vol. 64, no. 21, pp. 2284–2286, 2010.

[10] T. Jia, W. Wang, F. Long, Z. Fu, H. Wang, and Q. Zhang, "Synthesis, characterization and luminescence properties of Y-doped and Tb-doped ZnO nanocrystals," *Materials Science and Engineering B*, vol. 162, no. 3, pp. 179–184, 2009.

[11] R. Kaur, A. V. Singh, K. Sehrawat, N. C. Mehra, and R. M. Mehra, "Sol-gel derived yttrium doped ZnO nanostructures," *Journal of Non-Crystalline Solids*, vol. 352, pp. 2565–2568, 2006.

[12] Y. Natsume, H. Sakata, T. Hirayama, and H. Yanagida, "Low-temperature conductivity of ZnO films prepared by chemical vapor deposition," *Journal of Applied Physics*, vol. 72, no. 9, pp. 4203–4207, 1992.

[13] J. P. Xu, S. B. Shi, X. S. Zhang, Y. W. Wang, M. X. Zhu, and L. Li, "Structural and optical properties of (Al, K)-co-doped ZnO thin films deposited by a sol-gel technique," *Materials Science in Semiconductor Processing*, vol. 16, no. 3, pp. 732–737, 2013.

[14] J. Aranovich, A. Ortiz, and R. H. Bube, "Optical and electrical properties of ZnO films prepared by spray pyrolysis for solar cell applications," *Journal of Vacuum Science & Technology*, vol. 16, no. 4, pp. 994–1003, 1979.

[15] X. R. Ye, D. Z. Jia, J. Q. Yu, X. Q. Xin, and Z. L. Xue, "Fabrication and characterization of carbon nanotube/poly(vinyl alcohol) composites," *Advanced Materials*, vol. 11, no. 11, pp. 937–941, 1999.

[16] S. K. Mishra, R. K. Srivastava, S. G. Prakash, R. S. Yadav, and A. C. Pandey, "Direct acceleration of an electron in infinite vacuum by a pulsed radially-polarized laser beam," *Opto-Electronics Review*, vol. 18, no. 4, pp. 467–473, 2010.

[17] P. J. Yao, J. Wang, W. L. Chu, and Y. W. Hao, "Preparation and characterization of $La_{1-x}Sr_xFeO_3$ materials and their formaldehyde gas-sensing properties," *Journal of Materials Science*, vol. 48, no. 1, pp. 441–450, 2013.

[18] J. Huang, Y. Wu, C. Gu et al., "Large-scale synthesis of flowerlike ZnO nanostructure by a simple chemical solution route and its gas-sensing property," *Sensors and Actuators B*, vol. 146, no. 1, pp. 206–212, 2010.

[19] L. L. Yang, Q. X. Zhao, and M. Willander, "Size-controlled growth of well-aligned ZnO nanorod arrays with two-step chemical bath deposition method," *Journal of Alloys and Compounds*, vol. 469, no. 1-2, pp. 623–629, 2009.

[20] L. Yang, D. Qiu, F. Yu, S. Chen, and Y. Yin, "3D flowerlike ZnO micro-nanostructures via site-specific second nucleation in the zincethylenediaminehexamethylenetetramine tertiary system," *Materials Science in Semiconductor Processing*, vol. 14, no. 3-4, pp. 193–198, 2011.

[21] N. Yamazoe, J. Fuchigami, M. Kishikawa, and T. Seiyama, "Interactions of tin oxide surface with O_2, H_2O And H_2," *Surface Science*, vol. 86, pp. 335–344, 1979.

[22] J. Herrán, O. Fernández-González, I. Castro-Hurtado, T. Romero, G. G Mandayo, and E. Castaño, "Photoactivated solid-state gas sensor for carbon dioxide detection at room temperature," *Sensors and Actuators B*, vol. 149, no. 2, pp. 368–372, 2010.

[23] M. Ghasdi and H. Alamdari, "CO sensitive nanocrystalline $LaCoO_3$ perovskite sensor prepared by high energy ball milling," *Sensors and Actuators B*, vol. 148, no. 2, pp. 478–485, 2010.

[24] G. Sakai, N. Matsunaga, K. Shimanoe, and N. Yamazoe, "Theory of gas-diffusion controlled sensitivity for thin film semiconductor gas sensor," *Sensors and Actuators B*, vol. 80, no. 2, pp. 125–131, 2001.

[25] Q. Wan, Q. H. Li, Y. J. Chen et al., "Fabrication and ethanol sensing characteristics of ZnO nanowire gas sensors," *Applied Physics Letters*, vol. 84, no. 18, pp. 3654–3656, 2004.

[26] Y. Shimizu, S. Kai, Y. Takao, T. Hyodo, and M. Egashira, "Correlation between methylmercaptan gas-sensing properties and its surface chemistry of SnO_2-based sensor materials," *Sensors and Actuators B*, vol. 65, no. 1, pp. 349–357, 2000.

[27] C. Peng and Y. L. Liu, "Enhanced acetone sensing characteristics by decorating nanoparticles on ZnO flower-like structures," *Applied Physics A*, vol. 111, no. 4, pp. 1151–1157, 2013.

[28] M. Takata, D. Tsubone, and H. Yanagida, "Dependence of electrical conductivity of ZnO on degree of sintering," *Journal of the American Ceramic Society*, vol. 59, no. 1-2, pp. 4–8, 1976.

[29] M. E. Franke, T. J. Koplin, and U. Simon, "Metal and metal oxide nanoparticles in chemiresistors: does the nanoscale matter?" *Small*, vol. 2, pp. 36–50, 2006.

[30] X. C. Wang, M. G. Zhao, F. Liu, J. F. Jia, X. J. Li, and L. L. Gao, "C_2H_2 gas sensor based on Ni-doped ZnO electrospun nanofibers," *Ceramics International*, vol. 39, no. 3, pp. 2883–2887, 2013.